Journal of Sound and Vibration (1998) **217**(1), 17–31
Article No. sv981733

A NEW GOLF-SWING ROBOT MODEL UTILIZING SHAFT ELASTICITY

S. SUZUKI

Department of Mechanical System Engineering, *Kitami Institute of Technology*, *Kitami* 090-8507, *Japan*

AND

H. INOOKA

Department of System Information Science, *Tohoku University*, *Sendai* 980-0845, *Japan*

(*Received* 5 *February* 1998, *and in final form* 7 *April* 1998)

The performance of golf clubs and balls is generally evaluated by using golf-swing robots that conventionally have two or three joints with completely interrelated motion. This interrelation allows the user of this robot to specify only the initial posture and swing velocity of the robot and therefore the swing motion of this type of robot cannot be subtly adjusted to the specific characteristics of individual golf clubs. Consequently, golf-swing robots cannot accurately emulate advanced golfers, and this causes serious problems for the evaluation of golf club performance. In this study, a new golf-swing robot that can adjust its motion to both a specified value of swing velocity and the specific characteristics of individual golf clubs was analytically investigated. This robot utilizes the dynamic interference force produced by its swing motion and by shaft vibration and can therefore emulate advanced golfers and perform highly reliable evaluations of golf clubs.

1. INTRODUCTION

The dynamics of swing motion have been studied for many years in an effort to improve the performance of golf clubs and to optimize the swing of golf players [1–5]. Most of these analytical studies have focused on the double pendulum model of golf-swing motion and have taken into consideration only the shoulder and wrist joint movements of a golfer, while regarding the golfer's arms and golf club shaft as rigid rods. However, the vibration of the club shaft during the swing is also closely related to the golfer's motion, and the displacement of shaft vibration at impact greatly affects the trajectory of a hit ball. Therefore, advanced golfers pay a lot of attention to the flexural and torsional rigidity of the shaft. However, only a few studies have considered shaft vibration during the swing in order to optimize the design of a club shaft [6] and to control the golf-swing robot [7]. On the other hand, the golfer's skill and the accompanying interference drive of the golfer's joints are not examined [6].

0022–460X/98/410017 + 15 $30.00/0

Golf-swing robots are currently used to evaluate the performance of golf clubs and balls. Many of the golf-swing robots on the market have only two or three joints that are connected by gears and belts with completely interrelated motion. Therefore, although the user can adjust the initial posture and swing velocity of the robot, the swing motion cannot be adjusted according to the specific characteristics of individual golf clubs. Consequently, the robots often differ substantially from advanced golfers in the evaluation of golf clubs. One study on golf-swing robots applied the analytical results of human nailing motion to the down swing in order to examine the interference drive of a wrist joint using centrifugal force, Corioli's force and gravity [8]. However, the dynamic interference force due to shaft vibration, which may produce a comparatively large amount of interference, is not considered.

In the present study, a golf-swing robot that uses the dynamic interference force produced by the swing motion and the shaft vibration was analytically investigated. For this investigation, it was assumed that a skilful golfer can achieve fast head speed with less power by utilizing the dynamic interference force. The robot used in this study allows the swing motion to be planned according to the specific characteristics of a given golf club, such as the moment of inertia around the grip of a club and the flexural rigidity of the shaft. Using a simplified dynamic model, it was also investigated whether the torque-input at the shoulder could be determined when the head velocity at impact was specified for different types of clubs. Finally, this robot was compared with the conventional type of robot in terms of displacement of shaft vibration at impact and torque-input at the joints.

2. MODELLING

2.1. DYNAMIC MODEL

As shown in Figure 1, the entire golf-swing motion is assumed to occur in one plane. In the fixed co-ordinate system O–XYZ, the swing plane is inclined at an angle α to the X–Z plane. Usually, the value of α differs according to the golfer's physique and the club number. In the present study, the value of α was set at $\pi/3$ rad. The arm, club grip, and grip-holding fingers are regarded as independent rigid rods. Hereafter, the grip refers to the club grip, includng the grip-holding fingers, and impact means that a club head hits a ball.

Figure 2 shows the details of the dynamic model and co-ordinate systems. In this figure, the golf club head and shaft are referred to as the head and shaft, respectively. The shoulder joint rotates around the origin O of the co-ordinate system fixed on the swing plane and the wrist is considered as a passive joint containing only a brake mechanism, as the joint is either only fixed or released. The rotational co-ordinate system O'–xy is set using the end of the grip as the origin. The displacement of the shaft vibration is represented as $y(x, t)$. The angle of the arm with the X_0 axis is θ_1 and the angle of the grip with the X_0 axis is θ_2.

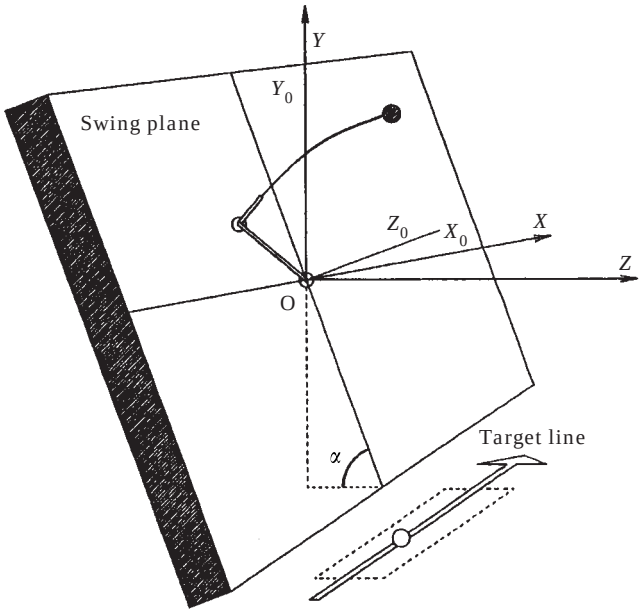

Figure 1. Plane of swing motion.

2.2. EQUATIONS OF MOTION

The equations of motion can be derived by applying Hamilton's principle to the dynamic model. Here, the friction of each section is ignored and it is assumed that the brake at the wrist joint can be fixed and released immediately. The centre of gravity of the head is assumed to be on the central axis of the shaft. Therefore,

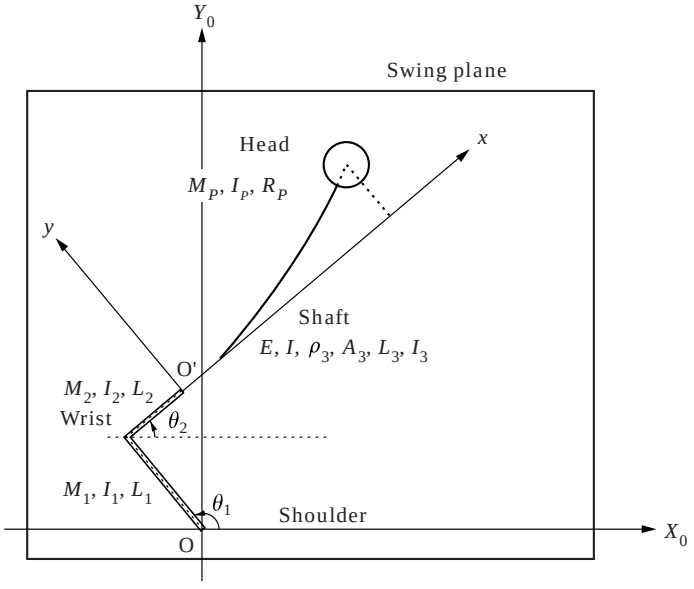

Figure 2. Co-ordinate systems of a golf-swing robot.

only the flexural vibrations on the swing plane about the shaft are considered. If the torque-input at the shoulder joint is Q_1 and at the wrist joint Q_2, the equations of motion are given as a balancing equation of moment at the shoulder joint (1), at the wrist joint (2), and an equation of the flexural vibration of the shaft (3).

$$C_1\ddot{\theta}_1 + (C_2L_C + D_1L_S)\ddot{\theta}_2 + (C_2L_S - D_1L_C)\dot{\theta}_2^2 + 2\dot{D}_1L_S\dot{\theta}_2 + \ddot{D}_1L_C + G_1\cos\theta_1 - Q_1 = 0, \tag{1}$$

$$(C_2L_C + D_1L_S)\ddot{\theta}_1 + (C_3 + D_2)\ddot{\theta}_2 - (C_2L_S - D_1L_C)\dot{\theta}_1^2 + 2D_3\dot{\theta}_2 + D_4 + G_2\cos\theta_2 - S_1\sin\theta_2 - Q_2 = 0, \tag{2}$$

$$\rho_3A_3L_C\ddot{\theta}_1 + \rho_3A_3(L_2 + x)\ddot{\theta}_2 - \rho_3A_3L_S\dot{\theta}_1^2 - \rho_3A_3y\dot{\theta}_2^2 + \rho_3A_3\ddot{y} + EIy'''' = 0. \tag{3}$$

The boundary conditions at the head of the golf club are

$$M_PL_C\ddot{\theta}_1 + M_PL_R\ddot{\theta}_2 - M_PL_S\dot{\theta}_1^2 - M_Py_P\dot{\theta}_2^2 + M_P\ddot{y} - EI'''_{L_3} = 0, \tag{4}$$

$$M_PR_PL_C\ddot{\theta}_1 + (M_PR_PL_R + I_P)\ddot{\theta}_2 - M_PR_PL_S\dot{\theta}_1^2 - M_PR_Py_P\dot{\theta}_2^2 + M_PR_P\ddot{y}_P + I_p\ddot{y}'_{L_3} + EIy''_{L_3} = 0. \tag{5}$$

Here, $\ddot{\theta} \equiv \mathrm{d}^2\theta/\mathrm{d}t^2$, $\ddot{y}' \equiv \partial^3 y/\partial t^2\,\partial x$, and so on. The symbols used in the equations are defined as

$$L_C = L_1\cos(\theta_1 - \theta_2), \qquad L_S = L_1\sin(\theta_1 - \theta_2), \qquad L_R = L_2 + L_3 + R_P,$$

$$y_{L_3} = y(L_3, t), \qquad M_3 = \rho_3A_3L_3,$$

$$C_1 = I_1 + (M_2 + M_3 + M_P)L_1^2, \qquad C_2 = \tfrac{1}{2}M_2L_2 + M_3(L_2 + \tfrac{1}{2}L_3) + M_PL_R,$$

$$C_3 = I_2 + I_3 + I_P + M_3L_2(L_2 + L_3) + M_PL_R^2,$$

$$D_1 = \rho_3A_3\int_0^{L_3} y\,\mathrm{d}x + M_Py_P, \qquad D_2 = \rho_3A_3\int_0^{L_3} y^2\,\mathrm{d}x + M_Py_P^2,$$

$$D_3 = \rho_3A_3\int_0^{L_3} y\dot{y}\,\mathrm{d}x + M_Py_P\dot{y}_P,$$

$$D_4 = \rho_3A_3\int_0^{L_3} (L_2 + x)\ddot{y}\,\mathrm{d}x + M_PL_R\ddot{y}_P + I_P\ddot{y}'_{L_3},$$

$$G_1 = (\tfrac{1}{2}M_1 + M_2 + M_3 + M_P)L_1g\sin\alpha,$$

$$G_2 = (\tfrac{1}{2}M_2L_2 + M_3L_2 + M_PL_R + \tfrac{1}{2}\rho_3A_3L_3^2)g\sin\alpha,$$

$$S_1 = \left(\rho_3A_3\int_0^{L_3} y\,\mathrm{d}x + M_Py_P\right)g\sin\alpha.$$

Using the eigenfunction of a cantilever $\varphi_i(x)$ that has a mass at the tip with no damping and the time function $q_i(t)$, the displacement of the shaft vibration can be approximated as

$$y(x, t) = \sum_{i=1}^{\infty} \varphi_i(x) q_i(t). \tag{6}$$

The expression of orthogonal conditions between modes with Kronecker's symbol is

$$\rho_3 A_3 \int_0^{L_3} \varphi_i(x)\varphi_j(x)\,\mathrm{d}x + M_p[\varphi_i(L_3)\varphi_j(L_3) + R_p\{\varphi_i(L_3)\varphi_j'(L_3) + \varphi_i'(L_3)\varphi_j(L_3)\}]$$

$$+(M_p R_p^2 + I_p)\varphi_i'(L_3)\varphi_j'(L_3) = \delta_{ij} \times M_3. \tag{7}$$

By applying this expression to equations (1)–(6), and by approximating the displacement of the shaft vibration to the secondary mode, the equation of motion becomes

$$\mathbf{J}\ddot{\mathbf{v}} + \mathbf{h} + \mathbf{g} = \mathbf{p}\mathbf{u},$$

$$\mathbf{J} = \begin{bmatrix} J_{11} & J_{12} & J_{13} & J_{14} \\ J_{12} & J_{22} & J_{23} & J_{24} \\ J_{13} & J_{23} & M_3 & 0 \\ J_{14} & J_{24} & 0 & M_3 \end{bmatrix}, \quad \mathbf{v} = [\theta_1 \quad \theta_2 \quad q_1 \quad q_2]^T, \quad \mathbf{h} = [h_1 \quad h_2 \quad h_3 \quad h_4]^T,$$

$$\mathbf{g} = [g_1 \;\; g_2 \;\; g_3 \;\; g_4]^T, \qquad \mathbf{p} = \begin{bmatrix} 1 & 0 & 0 & 0 \\ 0 & 1 & 0 & 0 \end{bmatrix}^T, \qquad \mathbf{u} = [Q_1 \;\; Q_2]^T,$$

where $\mathbf{J}$ is an inertia matrix, $\mathbf{h}$ is a vector of non-linear force, $\mathbf{g}$ is a vector of gravity, and $\mathbf{u}$ is an input vector.

Because the wrist is made passive in order to utilize the dynamic interference force, $Q_2 = 0$ while the joint is released and the dynamic model becomes a one-joint model while the joint is fixed. In order to simplify the calculation of the swing motion, all L_S about non-linear force is ignored. Using the derived equations of motion, the robotic swing motion is analyzed numerically using the fourth-degree Runge–Kutta method at intervals of $1{\cdot}0 \times 10^{-8}$.

3. MOTION SETTING

3.1. GOLFER'S SKILL

In order to investigate the degree to which the robot can emulate advanced golfers, it was assumed that the golfer had the ability to: adjust the swing motion to the characteristics of golf clubs; effectively utilize dynamic interference force; effectively utilize elasticity of the club shaft; achieve fast head speed with less power.

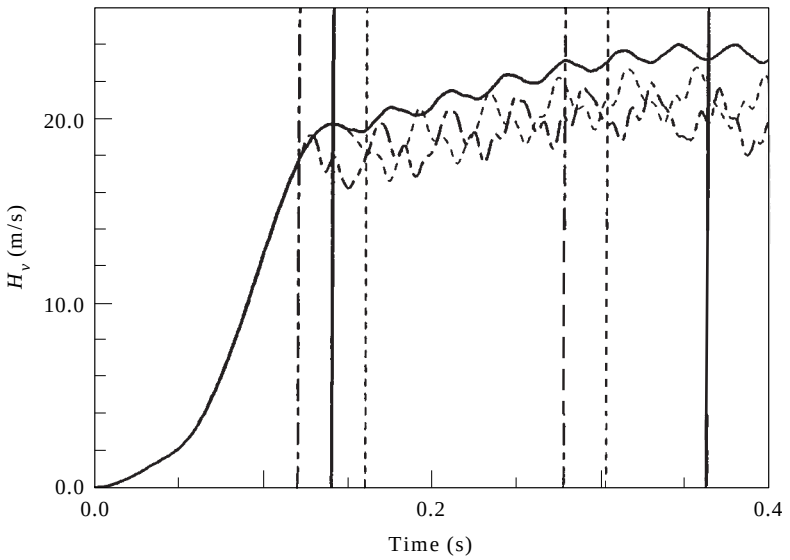

Figure 3. Comparison of head velocity for various release timings of the wrist joint. Release time (s): –·–, 0·12; ——, 0·14; ----, 0·16.

3.2. POSTURE AT START AND IMPACT INSTANT

In general, golfers twist the upper half of their bodies around the backbone during the swing motion. However, the dynamic model requires these motions to be substituted for rotation of the shoulder joint. Therefore, θ_1 is initially set at $\pi/2$ rad and θ_2 at 0. Because the central axes of the arm and grip are expected to point downward along the Y_0 axis at impact, both θ_1 and θ_2 are set at $3\pi/2$ rad.

3.3. RELEASE OF WRIST JOINT

The wrist joint of the robot is fixed at the beginning of the swing and is released during the swing. Many golf guide books note that the higher the golfer's skill, the later the wrist joint is released. Since advanced golfers pay much attention to the rigidity of a club shaft, simulation of the robotic swing motion was carried out by noting the relationship between shaft vibration and the time of release of the wrist joint. Based on the displacement of the shaft vibration, the release timing of the wrist joint was varied and the subsequent head velocity at impact was analyzed. The head velocity refers to the velocity at the centre of gravity of a club head on the fixed co-ordinate system O–XYZ.

The basic release timing is set at 140 ms after the start of the swing when the displacement of the shaft vibration zero-crosses in the positive direction for the first time. Two more release timings are set at 20 ms before and after the basic release timing. The maximum torque-input at the shoulder joint is set at 100 N · m for 50 ms. The acceleration time from the start of the swing is set for 116 ms. Figure 3 shows the results of a comparison of head velocity (H_V) for various release timings of the wrist joint. Releasing the wrist joint at the positive zero-cross point of the shaft vibration maximized the H_V. The posture at impact satisfied the conditions determined in section 3.1 only when the release timing was 140 ms after

the start of the swing. With respect to other release timings, the impact time refers to when the centre of a club head passes the Y_0 axis. The H_V curves indicate that even a difference of only 20 ms in release timing greatly affects the H_V.

The H_V curves of rigid and flexible shafts were also compared (Figure 4). This comparison was based on the above-mentioned setting. The thin solid line in the figure shows the H_V of the club with a rigid shaft under the same torque-input at the shoulder as a flexible shaft. The dashed and single-dotted line shows the H_V with a rigid shaft adjusting to make the H_V at impact almost equal to that of a club with a flexible shaft. The results of this analysis indicate that the same amount of torque at the shoulder accelerates the rotation of this joint only a little in the case of rigid shaft because no elasticity is available to reduce the torque. Consequently, the H_V becomes very slow. The maximum torque-input at the shoulder joint was 100 N · m for a flexible shaft but 150 N · m for a rigid shaft when the head velocities for both clubs were almost equal. Thus, a large torque is required if no elasticity is available. In the case of a rigid shaft, the arm goes ahead of the shaft during the swing (i.e., θ_1 is larger than θ_2). Thus, in order to correctly adjust the posture at impact, the shoulder joint would need to decelerate before impact as was also described in reference [8]. However, such an action does not occur during the golfer's swing motion with all their might.

These results indicate that shaft vibration is an important factor to consider when studying golf-swing robots, because advanced golfers may be effectively utilizing shaft elasticity to achieve good results. Therefore, the wrist joint should be released when the displacement of the shaft vibration zero-crosses in the positive direction for the first time after the start of the swing. Once fulfilled, this

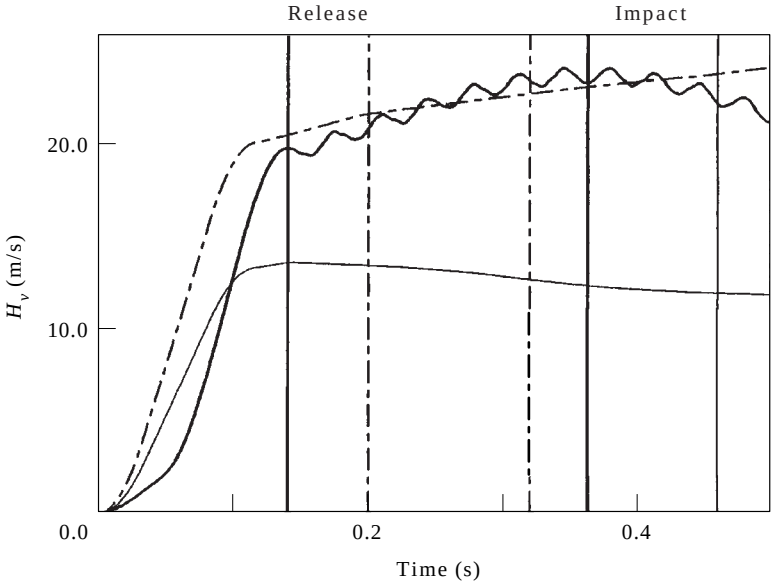

Figure 4. Comparison between head velocity of the club with a rigid shaft and with a flexible shaft. ——, Flexible shaft; ——, rigid shaft (under same conditions); — –, rigid shaft (under modified conditions).

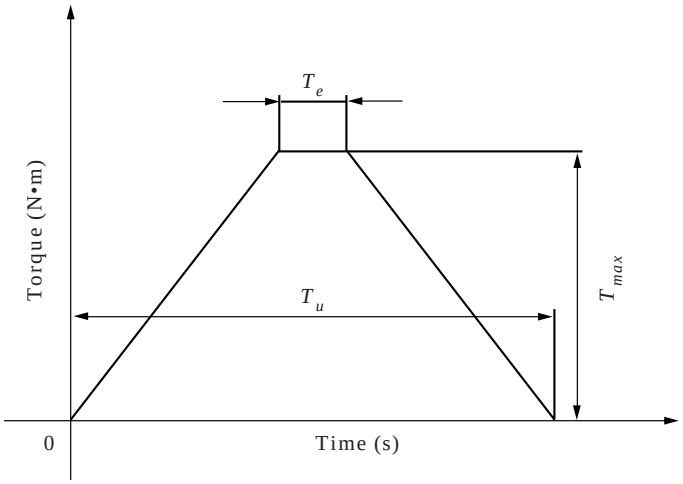

Figure 5. Torque function of the shoulder joint.

condition should reduce the differences between the evaluation of golf clubs by advanced golfers and by golf-swing robots.

4. TORQUE PLANNING

4.1. TORQUE FUNCTION

Usually golf-swing robots are commanded to maintain a specified head velocity at impact. However, the robot used in the present study is driven only by a dynamic interference force after the acceleration of the shoulder. Consequently, if many torque function variables have to be considered, torque planning will be difficult. In the present study, the torque function was set as a trapezoid (Figure 5). The swing motion is adapted to the moment of inertia around the grip of a club and flexural rigidity of the shaft by adjusting the height (T_{max}) and the bottom length (T_u) of the trapezoid. T_u determines the acceleration time of the shoulder joint, and T_{max} corresponds to the maximum muscular strength of the shoulder. The top length (T_e) corresponds to the duration of T_{max}. Because the duration in human golf-swing motion is comparatively short and does not differ greatly among individuals, the duration T_e was fixed at 50 ms.

TABLE 1

Specifications of the dynamic model

	Arm	Grip	Shaft	Head
L_1, L_2, L_3, R_P (m)	0·4	0·1	1·0	$2{\cdot}5 \times 10^{-2}$
M_1, M_2, M_3, M_P (kg)	5·0	1·0	$7{\cdot}5 \sim 12 \times 10^{-2}$	$2{\cdot}0 \sim 2{\cdot}5 \times 10^{-1}$
I_1, I_2, I_3, I_P (kg · m^2)	$2{\cdot}7 \times 10^{-1}$	$3{\cdot}3 \times 10^{-3}$	$2{\cdot}5 \times 10^{-2}$	$7{\cdot}5 \times 10^{-6}$

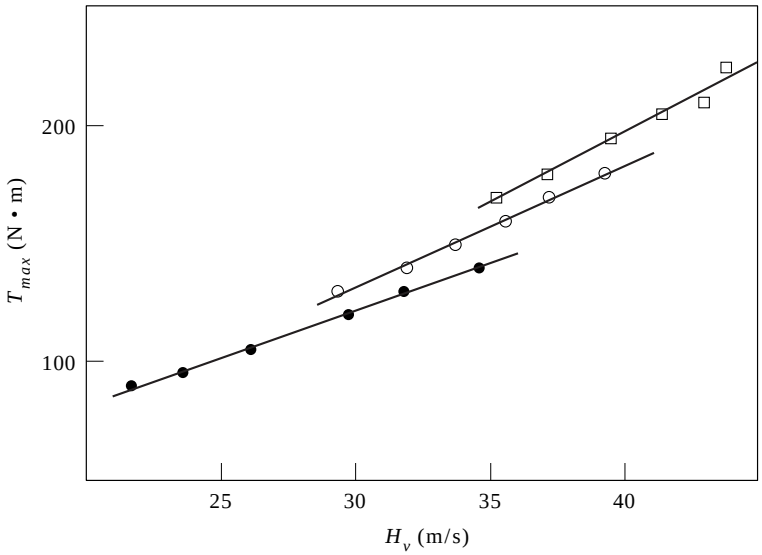

Figure 6. Relationship between head velocity at impact and T_{max} for three types of EI ($I_c = 2{\cdot}27 \times 10^{-1}$). —●—, $EI = 70$; —○—, $EI = 90$; —□—, $EI = 110$.

4.2. DETERMINATION OF TORQUE FUNCTION PARAMETERS

Table 1 lists the specifications of the dynamic model. The golf club has a spherical head of $5{\cdot}0 \times 10^{-2}$ m in diameter and a 1·0-m-long shaft that has uniform flexural rigidity along its entire length. The flexural rigidity of the shaft in the swing plane (EI) is set to range between 70 and 110 N · m^2. The moment of inertia of the club around the grip (I_c) is set to range between $2{\cdot}27 \times 10^{-1}$ and $2{\cdot}78 \times 10^{-1}$ kg · m^2. For setting the I_c range, the mass is assumed to be $7{\cdot}5 \times 10^{-2}$ to $1{\cdot}2 \times 10^{-1}$ kg for the shaft and $2{\cdot}0 \times 10^{-1}$ to $2{\cdot}5 \times 10^{-1}$ kg for the head. When the head velocity is specified using the above conditions, the torque function is determined as explained below.

Figure 6 shows the relationship between H_V and T_{max} for three types of EI (i.e., three types of clubs). For this analysis, I_c was fixed at $2{\cdot}27 \times 10^{-1}$ kg · m^2 and T_u was adjusted accurately to satisfy the conditions of motion. The relationship between H_V and T_{max} is approximately linear for each of the three types of clubs. Using these relationships, T_{max} can be defined for a specified head velocity using EI and I_c of the club. The greater the EI value, the higher the ranges of H_V and T_{max} that satisfy the conditions of the swing motion. This confirms the popular view that a stiff shaft is suitable for a muscular golfer who attains a fast head velocity.

Secondly, we determined the relationship between θ_{im} and T_u, where θ_{im} is the angle of the joint when θ_1 and θ_2 become equal during a swing. For this analysis, T_{max} was fixed at 100 N · m and I_c at $2{\cdot}27 \times 10^{-1}$ kg · m^2. Figure 7 shows the relationship between T_u and θ_{im} for three types of EI. The horizontal dashed line in the figure indicates the downward direction of the Y_0 axis. At impact, θ_{im} must satisfy this angle. This result shows that precise adjustment of T_u is very important to satisfy the conditions of motion because T_u greatly affects θ_{im}. Figure 8 shows the relationship between H_V and T_u for three types of I_c when EI is 70 N · m^2 and

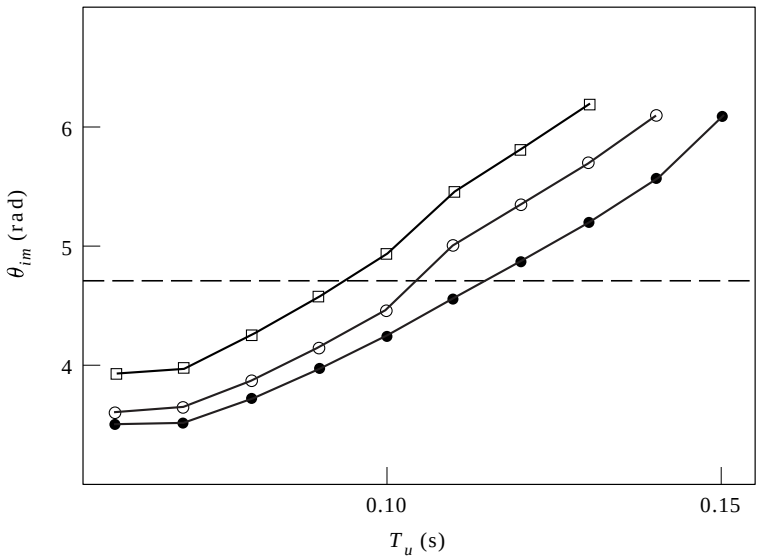

Figure 7. Relationship between T_u and θ_{im} for three types of EI ($T_{max} = 100$, $I_c = 2{\cdot}27 \times 10^{-1}$). —●—, $EI = 80$; —○—, $EI = 90$; —□—, $EI = 100$; ——, $\theta_1 = \theta_2 = 3\pi/2$ (rad).

T_{max} is 100 N · m. The relationship between H_V and T_u is also approximately linear. However, because the inclination of the plot is very small, changing the specified head velocity will not greatly affect T_u.

4.3. ALGORITHM

According to section 4.2, T_{max} and T_u can be defined by linear approximation. However, a relationship between T_{max} and T_u has yet to be established. Therefore,

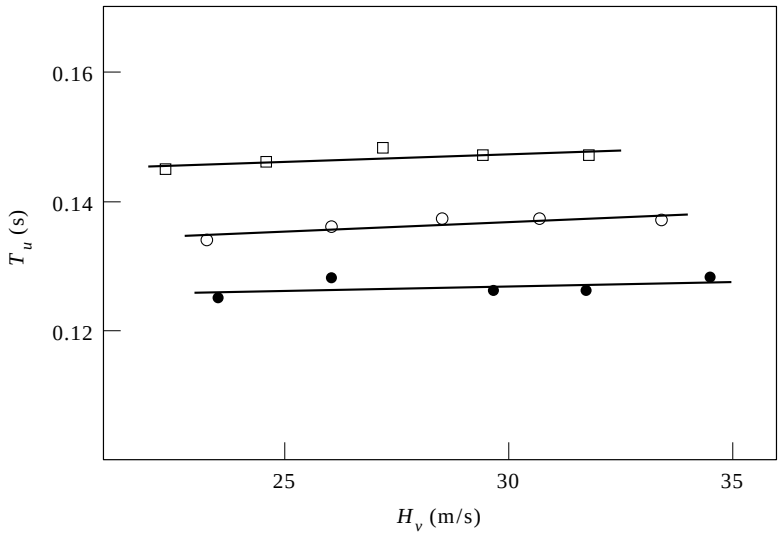

Figure 8. Relationship between head velocity at impact and T_u for three types of I_c ($EI = 70$, $T_{max} = 100$). —●—, $I_c = 2{\cdot}27 \times 10^{-1}$; —○—, $I_c = 2{\cdot}52 \times 10^{-1}$; —□—, $I_c = 2{\cdot}78 \times 10^{-1}$.

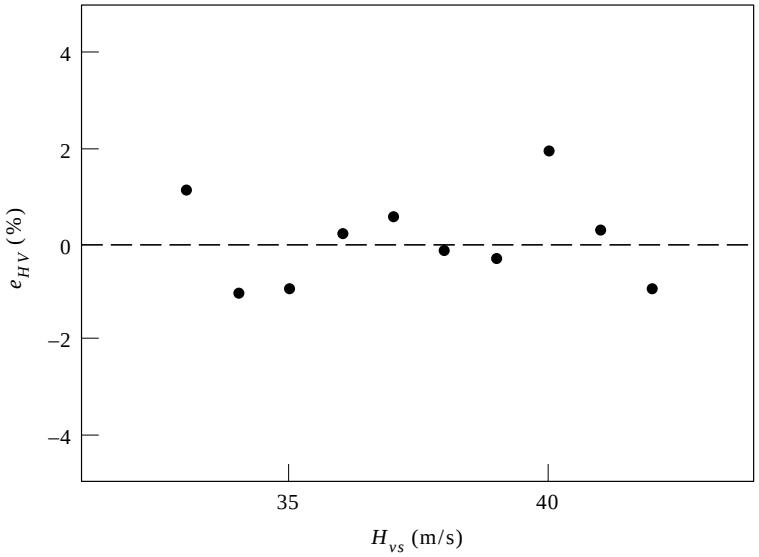

Figure 9. The error factor between head velocity and specified head velocity at impact ($EI = 100$, $I_c = 2{\cdot}27 \times 10^{-1}$).

an approximate value of T_u is tentatively determined first. By repeating the calculation at regular intervals using this value of T_u as the middle value, the value of T_u that satisfies the conditions of posture at impact is finally determined. This method is effective for adjusting the posture and is expected to reduce off-line calculation costs. The associated algorithm is as follows.

(1) Two linear expressions about T_u and T_{max} are selected from the EI and I_c of a given golf club. (2) A specified value of H_V is substituted into these linear expressions in order to determine T_{max} and to calculate an approximate T_u. (3) The calculation of swing motion is repeated five times at 1·0 ms intervals using the approximate value of T_u for the middle calculation. (4) The final T_u value is determined to maintain an error of θ_{im} within $\pm 3{\cdot}0 \times 10^{-2}$ rad.

5. SIMULATION OF ROBOTIC SWING MOTION

5.1. RELIABILITY OF SWING MOTIONS

The algorithm shown in section 4.3 gives priority to the setting conditions of θ_{im}, and thus an error may occur in the specified head velocity. Therefore, the reliability of the evaluation needs to be examined about H_V at impact. In this investigation, EI is set at 100 N · m^2 and I_c is $2{\cdot}27 \times 10^{-1}$ kg · m^2. The specified head velocity at impact is represented as H_{VS}. H_{VS} is varied at intervals of 1·0 m/s in the range of 33–42 m/s. The expression below represents the e_{HV} value (%), which indicates the error factor between H_V and H_{VS} at impact.

$$e_{HV} = 100 \times (H_V - H_{VS})/H_{VS}. \tag{8}$$

Figure 9 shows the results of this analysis. Because an error due to H_{VS} is always within $\pm 3{\cdot}0\%$, highly reliable evaluations can be expected. The stick picture in

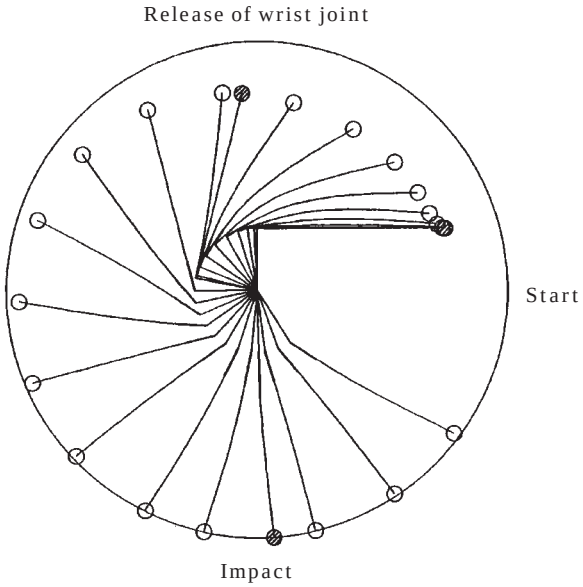

Figure 10. The stick picutre of the robotic swing motion ($H_{VS} = 35$).

Figure 10 shows the robotic swing motion when H_{VS} is set at 35 m/s. It was found that the torque plan according to the EI, I_c and H_{VS} satisfies the conditions of motion. If the identification of specific characteristics of individual golf clubs can be automated, the autonomous golf-swing motion can be adjusted correspondingly.

5.2. COMPARISON WITH THE CONVENTIONAL TYPE OF ROBOT

Displacement of shaft vibration greatly affects the trajectory of a hit ball because the displacement determines the face-angle of a club head at impact. This can cause serious problems in reliability of golf club evaluation by the conventional type of robot. In this regard, the proposed golf-swing robot, which is thought to be similar to the performance of an advanced golfer, seems to be different from the conventional type of robot. The displacements of shaft vibration in swing motion by the proposed robot (Type P) and two conventional types of robots were analyzed and compared. One conventional type of robot has servo motors and reducers at each joint (Type R) and the other has direct-drive actuators, for example, air cylinders or DC torque-motors and so on, without reducers (Type D). The actuators of Type D are controlled by the resolved-acceleration control method with non-linear and servo compensators for the path planning of angles and angular velocities of joints. It is assumed that Type R correctly maintains the path planning without being affected by dynamic interference because the reduction ratio at each joint is large. The path of θ_1 is planned as a linear expression and that of θ_2 is planned by two linear expressions before and after releasing the wrist joint. In this analysis, H_{VS} is set at 35 m/s and the value of EI was varied from 70 to 110 $\mathrm{N \cdot m^2}$ at intervals of 10 $\mathrm{N \cdot m^2}$.

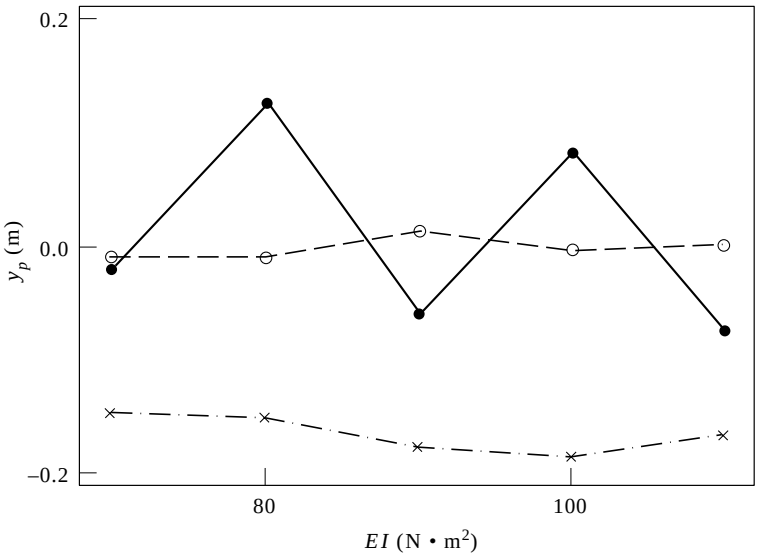

Figure 11. Comparison of y_p at impact for three types of robot ($H_{VS} = 35$). ●, Type P; ○, Type R; ×, Type D.

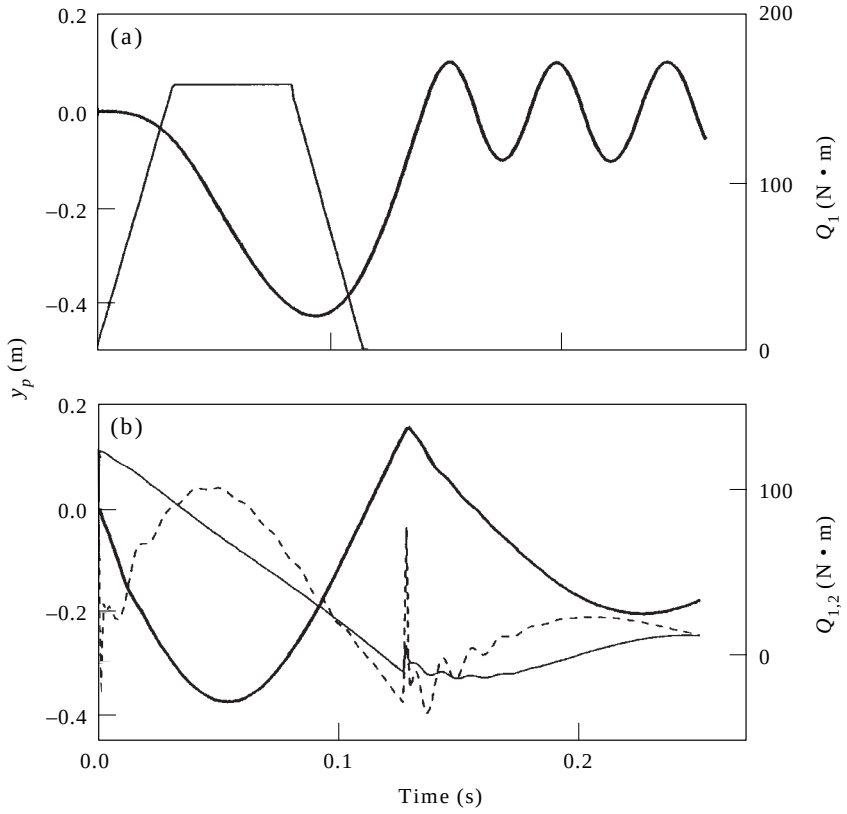

Figure 12. Comparison of the displacement of shaft vibration and torque-input ($H_{VS} = 35$, $EI = 100$). (a) Type P, (b) Type D. ——, y_p; ——, Q_1; ——, Q_2.

As shown in Figure 11, the displacement of Type P changes diversely for every EI. However, in the cases of Types R and D, the displacement is almost invariable because the wrist joint requires a large amount of toque-input at the release. Figure 12 shows a comparison of the displacement of shaft vibration and toque-input at each joint between Type P and Type D. It was found that Type D requires momentarily a large amount of torque at the start of the swing and the release of the wrist and that the displacement correspondingly becomes large. Consequently, the trajectory of a ball hit by the proposed robot and the conventional type of robot will be different even if H_V at impact is the same.

Similarly, in the analytical study on optimum design of golf clubs, as examined in reference [6], the paths of joint angles of a golfer need to be planned in consideration of the golfer's skill.

6. CONCLUSION

The following points summarize the results of our examination of a golf-swing robot that can adjust its swing motion according to the characteristics of any given golf club and to the specified head velocity.

In this model, releasing the wrist joint at the positive zero-cross point of the displacement of the shaft vibration maximizes the head velocity. This motion setting is expected to reduce the differences in the evaluation of golf clubs performed by advanced golfers and by the robot.

Once the torque function of the shoulder joint is set as a trapezoid, the height and the bottom length can be determined easily by off-line calculations. This trapezoid enables the swing motion to be easily adjusted according to the characteristics of a club and to a specified head velocity.

Although the algorithm for adjusting the swing motion gives priority to the setting of posture at impact, the error in head velocity does not exceed $\pm 3\%$. Thus, highly reliable evaluation of golf club performance can be expected.

The displacements of shaft vibration in swing motion by the proposed robot and conventional type of robot were different for all club shafts. Therefore, the trajectory of a ball hit by the proposed robot is expected to be similar to that hit by an advanced golfer.

Consequently, it is thought that the proposed robot can emulate the performance of advanced golfers and can therefore accurately evaluate golf club performance. Future research will focus on the verification of these results by experiments. It is expected that the dynamic model will be enhanced and that the effects of twisting motion of the wrist joint and torsional vibration of the shaft will be clarified.

REFERENCES

1. T. JORGENSEN 1970 *American Journal of Physics* **38**, 644–651. On the dynamics of the swing of a golf club.
2. M. A. LAMPSA 1975 *Transactions of the American Society of Mechanical Engineers, Journal of Dynamic Systems, Measurement, and Control* **75**, 362–367. Maximizing distance of the golf drive: an optimal control study.

3. D. R. Budney and D. G. Bellow 1982 *Research Quarterly for Exercise and Sport* **53**, 185–192. On the swing mechanics of a matched set of golf clubs.
4. P. D. Milburn 1982 *Medicine and Science in Sports and Exercise* **14**, 60–64. Summation of segmental velocities in the golf swing.
5. R. J. Neal and B. D. Wilson 1985 *International Journal of Sports and Biomechanics* **1**, 221–232. 3D Kinematics and kinetics of the golf swing.
6. T. Iwatsubo, N. Konishi and T. Yamaguchi 1990 *Transactions of the Japan Society of Mechanical Engineers C* **56**, 2386–2391. Research on optimum design of a golf club.
7. S. Suzuki and H. Inooka 1997 *Proceedings of* 6*th The Institute of Electrical and Electronics Engineers Workshop on Robot and Human Communication*, 28–33. Golf-swing robot emulating a human motion.
8. A. Ming, M. Kajitani, Z. Jin and K. Tsujihara 1995 *Preprint of the* 13*th Annual Conference of the Robotics Society of Japan* **3**, 1139–1140. Study on golf swing robot.

APPENDIX: NOTATION

M_1, M_2	mass of the arm and grip, respectively
M_p, R_p	mass and the radius of the club head, respectively
L_1, L_2	length of the arm and grip, respectively
L_3	length of the shaft
I_1	moment of inertia of the arm around the shoulder joint
I_2	moment of inertia of the grip around the wrist joint
I_3	moment of inertia of the shaft around the grip
I_p	moment of inertia of the club head
E, I	Young's modulus and second moment of area of the shaft, respectively
P_3, A_3	density and cross-section of the shaft, respectively